

WestminsterResearch

<http://www.westminster.ac.uk/westminsterresearch>

**Comparative Analysis of Micro/Minichannel Flow Boiling Pattern
Recognition and Classification using Clustering Algorithms
Mohammad Harris, Angelopoulou, A., Hongwei Wu and Wenbin
Zhang**

This is a copy of the author's accepted version of a paper subsequently published in the proceedings of the IEEE 14th International Conference on Pattern Recognition Systems (ICPRS), University of Westminster, London, 15-18 Jul 2024, IEEE.

The final published version will be available online at:

<https://ieeexplore.ieee.org/Xplore/home.jsp>

© 2024 IEEE. This manuscript version is made available under the CC-BY 4.0 license

<https://creativecommons.org/licenses/by/4.0/>

The WestminsterResearch online digital archive at the University of Westminster aims to make the research output of the University available to a wider audience. Copyright and Moral Rights remain with the authors and/or copyright owners.

Comparative Analysis of Micro/Minichannel Flow Boiling Pattern Recognition and Classification using Clustering Algorithms

Abstract—Microchannel heat sinks have attracted considerable attention in thermal management applications owing to their high heat transfer capabilities and compact size. Among the various cooling techniques, flow boiling in microchannels has emerged as a promising method for efficient heat dissipation. However, the intricate flow patterns in microchannels present challenges for accurate classification, pattern recognition, and inefficient data handling practices. This paper presented a comparative analysis of flow boiling classification techniques for pattern recognition in microchannel heat sinks. Three different clustering algorithm-driven convolutional neural networks (CNNs) were analysed and compared alongside a base CNN to establish a data pipeline capable of agile flow boiling pattern recognition. The Gaussian Mixture Model Clustering-based CNN exhibited the best performance, achieving an overall mean accuracy of 88% for the test set validation. Thus, this study lays the groundwork for improving the performance of flow boiling pattern recognition in microchannel heat sinks.

Index Terms—pattern recognition, image analysis, clustering algorithm, flow boiling, thermal management, case study

I. INTRODUCTION

Micro-technologies have become integral components of electronic devices in today's world. Microchannels fall among these technologies, employing narrow passages/lanes and exploiting high surface area-to-volume ratios to boost convective heat transfer. Thus, this makes them exceptionally effective for cooling applications in electronic gadgets, energy systems, and automotive and aerospace industries. Despite the array of cooling methods used in microchannel heat sinks, flow boiling remains one of the most promising techniques for achieving high heat transfer and optimal thermal performance [1].

The flow boiling mechanism involves intricate interactions between liquid and vapour phases, resulting in varied flow patterns and heat transfer dynamics within microchannel heat sinks. However, due to the complex interchange and physical phenomena involved, flow boiling classification contains many challenges related to subjectivity, interpretability, generalisability, and accuracy, amongst other issues [2]. Therefore, understanding and accurately categorising these flow patterns is crucial for enhancing heat transfer efficiency and ensuring dependable thermal management. Furthermore, classifying flow boiling regimes helps engineers to tailor microchannel designs to specific operational conditions, thereby maximising heat dissipation while minimising thermal resistance, pressure drops, or energy consumption.

Consequently, this study conducts a comparative assessment of flow boiling classification in micro/mini channel

heat sinks, employing neural network-based classification and pattern recognition via clustering algorithms under varying mass flow rate conditions (ranging from 180 mL/min to 600 mL/min). The research aims to offer a new perspective and evaluate different algorithms via a custom dataset gained from experimental findings; thus, the focus lies in assessing machine learning-based approaches, specifically clustering methods, for accurately recognising and labelling boiling patterns in microchannel heat sinks. Thus, the research provides the following major contributions:

- 1) A streamlined, generalisable flow boiling image segmentation pipeline;
- 2) A semi-automated system to generate data and classify images for flow boiling analysis;
- 3) A baseline boiling regime classifier using clustering that can be expanded/built upon;
- 4) A methodological comparative analysis of clustering algorithms not reported in similar preceding works;
- 5) Furthermore, the system considers a mixture of different bubble formations and regimes with data augmentations, so there is the generalisability of the proposed work in real-world applications such as different lighting conditions, backgrounds, and orientations.

This paper is structured as follows: Section 2 outlines the related work and strategies. Section 3 highlights the research methodology, the experimental setup, and data collection. Section 4 presents the outcomes of flow boiling classification and comparative analysis. Finally, the concluding section summarises the paper and highlights future avenues for research in flow boiling classification for microchannel heat sinks.

II. RELATED WORK

Reviewing the literature shows that boiling heat transfer classification, particularly in micro/mini channels, has various implications for diverse engineering applications. Flow boiling patterns directly impact heat transfer efficiency, system stability, and energy usage [3]. In micro/mini channels, where space constraints and high heat fluxes prevail, precise classification becomes even more critical for effective thermal management. Therefore, accurate classification of boiling heat transfer regimes is integral for optimising heat transfer processes, enhancing system performance, and ensuring operational safety. However, achieving robust classification methodologies in such intricate systems presents many challenges, warranting a critical review of existing techniques and further research.

The current flow pattern classification and recognition strategies encompass a spectrum of approaches ranging from traditional empirical correlations, computer vision and advanced machine learning algorithms. [4] Flow pattern detection methods can mainly be categorised into direct and indirect techniques. While direct methods, such as high-speed photography and X-ray computed tomography, provide intuitive insights into flow patterns, they can be subjective in their interpretation and often require manual feature extraction or data labelling. On the other hand, indirect methods, such as time-frequency analysis methods (TFA), can analyse fluctuation signals (such as pressure drop, flow, or electrical impedance) to identify flow patterns [5]. While TFA is a popular indirect method, other techniques include statistical analysis theories like probability density function (PDF). One of the main limitations of indirect methods like TFA is their sensitivity to noise and signal interference, making them unsuitable for accurately capturing the dynamics of complex systems such as flow boiling, ultimately leading to incorrect results.

Moreover, relying on traditional methods and empirical correlations may struggle to capture the intricate dynamics/changes of flow boiling phenomena, leading to limitations in accuracy and generalisation. The prospect of machine learning and deep learning algorithms has revamped flow boiling classification by offering data-driven, automated, and scalable solutions. Techniques like K-nearest neighbours (KNN), Random Forest, Support Vector Machine (SVM), and Multilayer Perceptron (MLP) have demonstrated promising results in classifying flow patterns based on diverse input parameters [?]. These algorithms leverage large datasets to uncover intricate patterns and relationships, enhancing classification accuracy and generalisation across different operational conditions. Nevertheless, the effectiveness of machine learning or deep learning-related pattern recognition or classification relies on several critical factors, including training data quality, feature selection, data labelling, and model robustness. Furthermore, the interpretability of machine learning models remains a concern, particularly in safety-critical applications where understanding classification decisions is crucial.

Clustering methods, such as K-means, Gaussian Mixture Models (GMM), and Hierarchical Clustering, are widely recognised unsupervised learning techniques extensively employed in pattern recognition tasks like image analysis [?]. Despite their popularity, they remain underutilised in flow boiling research, particularly in microchannel/minichannel studies. Recent research in this field has predominantly focused on bubble dynamics in flow boiling via chord lengths and bubble diameters [?]. However, boiling dynamics within a generalised system may significantly differ in micro-scale systems, necessitating more targeted investigations for a comprehensive analysis. Moreover, experimental data acquisition is costly, and large dataset-based artificial intelligence models demand considerable computational power and expenses. Therefore, there is a growing need for robust yet agile methods that address the current demands of rapid product development times — while minimising complexity and data requirements. Recent

reports suggest that smaller datasets, especially in the thermal management area, can yield superior results [9]. Accordingly, there is a prospect to leverage clustering techniques to extract meaningful insights from such datasets, potentially enhancing the understanding of flow boiling phenomena in microchannel and minichannel systems.

A. Clustering Algorithms for Flow Boiling

As previously highlighted, the three chosen clustering algorithms promise significant potential for advancing research in flow boiling pattern classification/recognition. While the definitions and intricacies of these methods are well-documented in existing literature [7, 10-11], a brief overview of their underlying mechanics and equations is provided in the following:

1. K-means Clustering: The k-means algorithm aims to segment/partition a given input dataset into k number of clusters, where each data point belongs to the cluster with the nearest mean. The algorithm iteratively optimises the position of the cluster centroids to minimise within-cluster sums of squared distances. The objective function for k-means can be expressed as:

$$\arg \min_{\mathbf{S}} \sum_{i=1}^k \sum_{\mathbf{x} \in S_i} \|\mathbf{x} - \mu_i\|^2$$

where: $\mathbf{S} = \{S_1, S_2, \dots, S_k\}$ represents the partitioning of the dataset into k clusters; μ_i is the centroid (mean) of cluster S_i ; $\|\mathbf{x} - \mu_i\|^2$ denotes the squared Euclidean distance between a data point \mathbf{x} and the centroid μ_i . The goal is to find the optimal partitioning \mathbf{S} and centroid positions $\{\mu_1, \mu_2, \dots, \mu_k\}$ that minimise the objective function. The algorithm iterates between two steps: assigning each data point to the nearest centroid to form clusters and updating the centroids based on the mean data points in each cluster.

The rationale behind choosing the k-means algorithm is that it can group similar patterns or features extracted from flow-boiling images. For instance, it can cluster images based on pixel intensities, texture features, or other image descriptors, helping identify different flow regimes or flow anomalies.

2. Gaussian Mixture Models (GMM): Gaussian Mixture Models (GMM) are a probabilistic model used for clustering tasks, where data points are assumed to arise from a mixture of several Gaussian distributions. The probability density function (PDF) of a GMM is given by the following equation:

$$p(\mathbf{x}) = \sum_{i=1}^k \phi_i \cdot \mathcal{N}(\mathbf{x} | \mu_i, \Sigma_i)$$

Where:

- \mathbf{x} represents the observed data point.
- k is the number of mixture components.
- ϕ_i is the mixing coefficient associated with the i^{th} Gaussian component, satisfying $\sum_{i=1}^k \phi_i = 1$.
- μ_i is the mean vector of the i^{th} Gaussian component.
- Σ_i is the covariance matrix of the i^{th} Gaussian component.

- $\mathcal{N}(\mathbf{x}|\boldsymbol{\mu}_i, \boldsymbol{\Sigma}_i)$ denotes the multivariate Gaussian distribution with mean $\boldsymbol{\mu}_i$ and covariance $\boldsymbol{\Sigma}_i$.

The parameters of the GMM, namely the mixing coefficients ϕ_i , means $\boldsymbol{\mu}_i$, and covariance matrices $\boldsymbol{\Sigma}_i$, are typically estimated using the Expectation-Maximisation (EM) algorithm. The EM algorithm iteratively optimises the parameters to maximise the likelihood of the observed data from the given model. Once trained, GMMs can assign clusters to data points based on their probability under each Gaussian component.

As GMM can model complex distributions in flow boiling images, it potentially enables the identification of different patterns or regions of interest. It can be applied to segment images into distinct regions based on pixel intensities or texture features (such as bubble formation or coalescence), aiding in feature extraction and subsequent recognition tasks.

3. Hierarchical Clustering: Hierarchical clustering, as the name suggests, is a method used to build a hierarchy of clusters, which can be visualised as a tree-like structure known as a dendrogram. There are two main types of hierarchical clustering: agglomerative and divisive. In this study, agglomerative hierarchical clustering will be investigated as it is more commonly used. Agglomerative hierarchical clustering starts with each data point in its cluster and then iteratively merges the closest clusters until only one cluster remains. The distance between clusters is often measured using a linkage criterion, such as the single linkage, complete linkage, or mean linkage. The linkage criterion defines the distance between two clusters A and B as:

$$d(A, B) = \min_{\mathbf{x} \in A, \mathbf{y} \in B} \text{dist}(\mathbf{x}, \mathbf{y})$$

where:

- A and B are two clusters being considered for merging.
- $\text{dist}(\mathbf{x}, \mathbf{y})$ is the distance between data points \mathbf{x} and \mathbf{y} .

Based on this linkage criterion, different distance measures such as Euclidean distance, Manhattan distance, or cosine similarity can be used to calculate $\text{dist}(\mathbf{x}, \mathbf{y})$.

Therefore, the agglomerative hierarchical clustering algorithm can then be summarised as follows:

- 1) Start with each data point in its cluster.
- 2) Compute the distance between all pairs of clusters.
- 3) Merge the two closest clusters.
- 4) Update the distance matrix.
- 5) Repeat steps 2-4 until only one cluster remains.

The dendrogram generated by hierarchical clustering visually represents the merging process and can be cut at different heights to obtain the desired number of clusters. Hierarchical clustering can reveal hierarchical structures in flow boiling images, identifying both macroscopic and microscopic patterns. Additionally, it can help understand relationships between different features or segments in the images, aiding in the interpretation and analysis of flow boiling phenomena.

Therefore, based on the discussion regarding the three chosen algorithms, it can be remarked that in flow boiling image pattern recognition, these clustering methods can preprocess

data by segmenting images into meaningful regions, extracting features, or reducing dimensionality. They can enable distinct flow regimes' identification, anomalies, or critical patterns, facilitating further analysis or decision-making processes in flow boiling systems.

III. MATERIALS AND METHODS

This paper presents an image analysis and pattern recognition study using a custom dataset derived from experimental findings. The process involves creating a data pipeline and synthetic datasets, detailed across subsequent sections covering data collection, augmentation, model construction, and evaluation. While other studies in extant literature have explored pattern recognition with custom datasets to create data pipelines for different applications [12], this research addresses challenges like subjectivity, feature extraction, and data labelling by comparing the performance of manually labelled flow boiling data and unlabelled clustering algorithm data through a clustering-based convolutional neural network (CNN) classification. Given the high costs of experimental investigations and diverse behaviours of flow boiling systems, custom datasets play a critical role in expanding research avenues and enhancing future pattern recognition techniques. Therefore, while ResNet50 or CIFAR10 datasets may yield good results elsewhere, using a custom dataset for training flow boiling images offers unique advantages: ensuring the model learns relevant features, adapts to image characteristics, and enables fine-tuning for optimal performance.

A. Data Acquisition and Experimental Setup

The experimental setup consists of a visual water-vapour two-phase flow boiling system designed to evaluate heat transfer and flow dynamics within narrow rectangular channels, particularly under various heat flux and mass flow rate conditions. The system comprises several components, including the experimental section, peristaltic pump, data tracker, control instrument, measurement apparatus, thermal bath, etc. Figure 1 illustrates the setup used for data collection, image credit: [13].

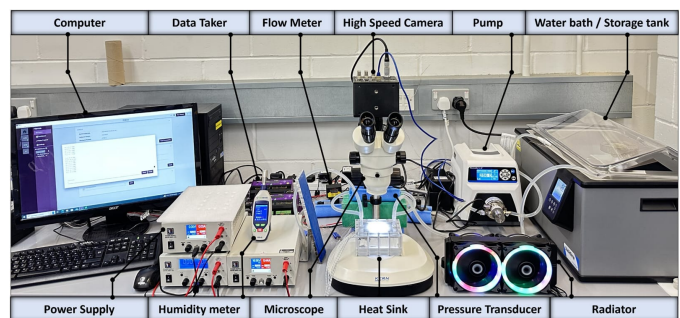


Fig. 1. Experimental setup

Looking at the equipment from the top left, starting with the computer, the desktop served as the base for initiating the experimental setup and storing images and other quantitative data related to heat transfer. The DT80 data tracker managed

data acquisition; its primary function was to detect temperature distribution along the microchannel heat sink, inlet and outlet of the system and monitor the subcooled temperature of the water bath. Additionally, a peristaltic pump was used to generate pumping power and circulate water along the pipes and channels; flow rates in the pipes were determined using an electromagnetic flowmeter and ranged from 180 mL/min to 600 mL/min. For this experiment, a thermal water bath was used to initiate and terminate the water flow loop in the system and subcool the working fluid. Deionized water served as the working fluid, circulated within the system via the main pump, and preheated to achieve a predetermined subcooling level in the thermal bath. Subsequently, it passes through the test section, initiating the boiling process. The resulting two-phase mixture ascends, undergoing cooling in an air-cooled radiator system before returning to the main pump, thus completing a closed-loop configuration.

Within the experimental section, narrow rectangular channels were horizontally positioned to facilitate flow and image capture. These channels, enveloped in 10mm thick acrylic for thermal insulation and protection, are constructed to ensure visibility. The channel area covers 80 mm x 60 mm, with a cross-sectional dimension of 2 mm x 2 mm per channel, heated by six RSPRO 300 W cartridge heaters using a 220 V power supply for controlled heating. The maximum heat flux that can be reached by the heaters was approximately 37.5 W/cm².

Measurement and monitoring were achieved through a suite of instruments. Temperature measurements utilize T-type thermocouples with an accuracy exhibiting an error margin of $\pm 0.5^{\circ}\text{C}$. Five thermocouples were evenly spaced across the heating base to ensure no heating hot spots were present that could affect the flow of boiling bubble formations, ultimately leading to incorrect results. An image acquisition system, consisting of a FASTCAM MINI UX-100 high-speed camera, and an optical microscope with an LED background light source was deployed. This entire system captured the evolution of various gas-liquid two-phase flow patterns during the experiment. Accordingly, four distinctive flow patterns were observed: dispersed bubbly flow (jets), bubble-slug flow, annular-like flow, and mist flow (local dry-out), as shown in Figure 2.

B. Dataset Description

In the classification of flow boiling regimes, several criteria are utilised to delineate distinct patterns and behaviours within the boiling process. These criteria encompass factors such as bubble size and distribution, the thickness of the liquid film surrounding bubbles, the presence of dry-out regions, and the overall flow dynamics observed. By analysing these parameters, researchers can categorise flow boiling regimes into different phases, each characterised by unique thermal and hydrodynamic properties. Identifying different flow regimes within a flow boiling system involves careful observation and analysis of several key characteristics unique to each regime. In general, flow boiling can be categorised into four broad categories [2]. Jet flow is typically characterised by the

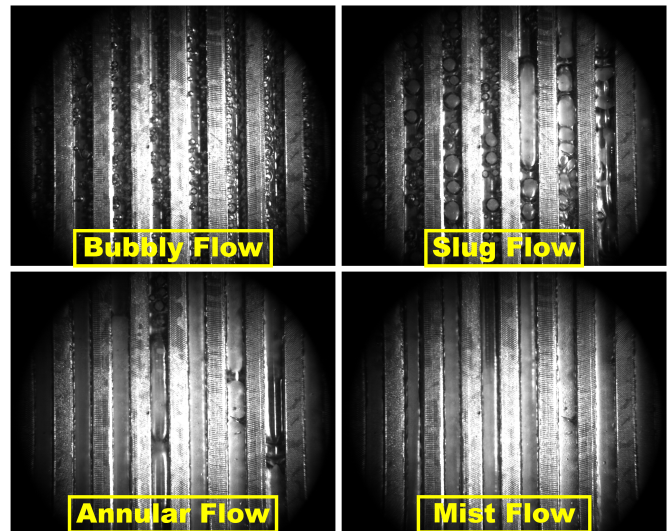


Fig. 2. Different flow regimes

presence of small, dispersed bubbles resembling jets within the liquid phase, while slug flow is marked by the alternating presence of elongated bubbles (slugs) and liquid slugs moving through the flow channel. Annular flow is distinguished by the formation of a continuous vapour phase surrounding a thin liquid film along the walls of the flow channel, and mist flow occurs when the liquid film becomes thin enough to expose patches of the wall directly to the vapour phase. In practice, distinguishing between these flow regimes often involves a combination of visual observation, analysis of flow patterns, measurement of bubble or slug sizes and velocities, and monitoring changes in local heat transfer rates.

The high-speed camera utilised in this study initially recorded videos capturing the entire duration of the boiling process. However, to focus on the analysis and extract meaningful insights, the authors specifically selected the first phase of boiling, spanning from the initiation of the jet-like dispersed bubbly flow to the occurrence of local dry-out regions. This selective approach allowed for a detailed examination of the critical transitional stages within the flow boiling process, shedding light on the mechanisms underlying heat transfer and vapour-liquid interactions. From the captured videos, 1600 images were extracted for further investigation. However, even with this meticulous approach, subtle changes in flow regime dynamics proved challenging to follow, emphasising the complexity of flow boiling phenomena and the necessity for advanced visualisation techniques and detailed analysis to unravel its intricacies accurately. Hence, through this targeted investigation, a deeper understanding of flow boiling and its practical implications in various engineering applications can be achieved.

C. Data Pipeline

The experimental setup generated data and was stored in a local dataset. To aid analysis, manual data labelling

was performed to distinguish between flow boiling regimes. Initially, the labelled datasets were used to construct the base Convolutional Neural Network (CNN) model, enabling an assessment of its accuracy. Following this, the base CNN model acted as a foundation for analysis and classification using clustering techniques. The raw data undergoes augmentation and progresses through feature mapping stages such as convolutional, pooling, flattening, and ultimately resulting in fully connected layers capable of enabling multi-class classification of flow boiling regimes.

Before augmentation, the images underwent resizing from 1280x1024 to 500x500. However, this reduction in dimensions resulted in a deterioration of image lighting. Thus, to rectify this issue and improve contrast, a Histogram equalization was applied. Regarding the convolutional layers, the initial layer comprised 64 filters, with each subsequent layer containing 32 filters. The stride size for each step was set to 2, and a max pooling of 2 was utilised. The image preprocessing phase was initiated with an image size of 224 and a batch size of 64. Following this, the images underwent augmentation, which included rescaling, zooming, shearing, and horizontal flipping. Given the significance of preserving bubble features, extensive noise or Gaussian augmentation was intentionally omitted. Figure 3 shows a sample data augmentation process.

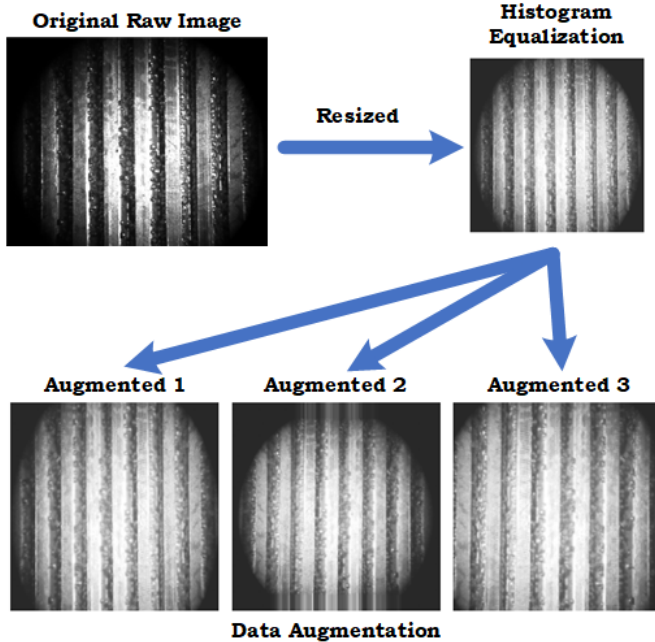


Fig. 3. Sample data augmentations

Furthermore, the dataset had a 90% training and 10% test split. This division aimed to maximise the effective utilisation of the dataset for training whilst ensuring reliable results on the test sets [14]. In real-life applications, test datasets often tend to be small — hence the rationale behind this choice. Additionally, the division ensures reliable evaluation by maintaining a separate test set to enable a realistic assessment of the model’s generalisation to unseen data; thus, replicating limited testing

scenarios helps simulate real-world conditions. Moreover, a smaller test set reduces the risks of overfitting, where the model may memorise training data. To address overfitting, techniques such as regularisation, dropout, or adjustment of model complexity can be employed later to optimise the best-performing model. The accuracy of the models and the loss function was assessed using the categorical cross-entropy loss (softmax loss) [15], which is typically defined as follows:

Given:

- y_i : the true label (ground truth) for sample i
- p_i : the predicted probability distribution over all classes for sample i
- N : the total number of samples
- C : the total number of classes

Then, the categorical cross-entropy loss L is calculated as:

$$L = -\frac{1}{N} \sum_{i=1}^N \sum_{c=1}^C y_{i,c} \cdot \log(p_{i,c})$$

where:

- $y_{i,c}$ is the indicator function, which is 1 if the true label of sample i is class c , and 0 otherwise.
- $p_{i,c}$ is the predicted probability of sample i belonging to class c according to the model’s output.

This loss function penalises models based on the difference between predicted probabilities and true labels across all classes, encouraging the model to assign high probabilities to the correct class labels.

The evaluation of the base CNN model was then carried out using the initial labelled data. Simultaneously, unlabelled data was fed into three distinct clustering algorithms, segmenting and classifying images into four distinct clusters for the four different flow regimes, with results stored in a desired local directory. The coding of the data pipeline facilitates clustering analysis and saves data, requiring minimal preprocessing and fostering agile analysis from experiments, leading to agile product development. With each iteration or data capture, new data seamlessly integrates to train clustering algorithms, allowing for semi-supervised generation and storage of synthetic data, pattern recognition, and organisation into four directories. This streamlined process significantly reduced the need for manual data handling, ensuring consistency between the root and save directories. The data pipeline loop, illustrated in Figure 4, underscores the iterative nature of the process. Subsequently, the clustered data was reintegrated into the base CNN setup to assess training and validation accuracy, thereby evaluating the feasibility and effectiveness of employing clustering-based pattern recognition to ultimately reduce the need for extensive manual labelling of future larger datasets.

IV. RESULTS AND DISCUSSION

A. CNN Classification

The experiment and images from Figure 2 highlight how the confined space within narrow channels restricts bubble

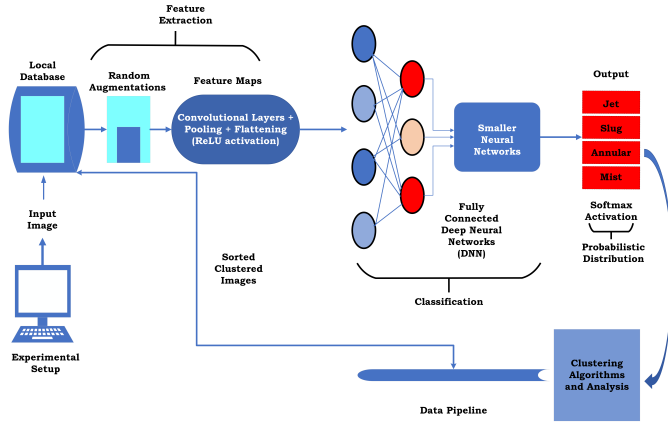


Fig. 4. Architecture for data pipeline and model implementations

development, altering bubble morphology compared to traditional tubes or pipes. The deformation or bursting of bubbles under different wall flow conditions significantly influences flow patterns and can produce mixed patterns. Consequently, labelling the data and flow patterns poses challenges and is subject to interpretability issues, affecting the accuracy of classification models and the usability of datasets for generalisation or specific applications. To further assess these challenges, initially, a convolutional neural network (CNN) was trained on the dataset, incorporating a fully connected layer along with two additional layers, and the model was further fine-tuned with additional epochs. Figure 5 illustrates the comparison of classification accuracy achieved by the CNN.

The results from the CNN indicate significant variations between each epoch, ranging from 10-50% for the base CNN model. Although the addition of extra layers or epochs improves the accuracy of the validation on test sets, the overall variation across different epochs keeps the reliability of the classification below 75%, dropping to lower than 70% for the other two models. These substantial variations or the zigzag pattern suggest the challenge for neural networks to consistently identify flow patterns accurately, indicating potential subjectivity and complexity issues in labelling datasets where one image could belong to multiple categories visually. While high accuracy values of 90% to 95% seem promising, they also imply overfitting problems based on the validation results, highlighting the need for a more objective assessment and methodology to enhance the classification robustness.

B. Clustering Implementation

Three different types of clustering algorithms were implemented. It can be seen that K-means has a relatively even distribution of cluster points where Hierarchical clustering heavily classifies one type of cluster more than the others. For the Gaussian model, cluster 3 contains the most points. The cluster outputs were then fed through the same base CNN model for classification comparison. The comparative analysis of flow boiling regimes across clustering algorithms

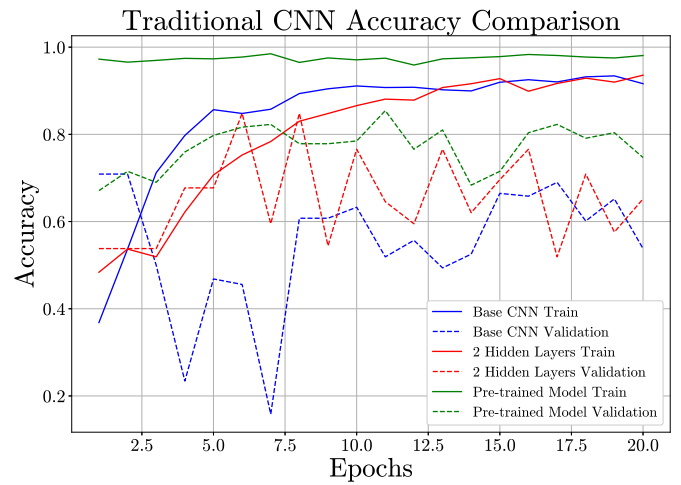


Fig. 5. CNN classification accuracy

yields interesting findings. Despite consistent total input counts of data points assigned to each algorithm, variations exist in how these points are distributed across clusters, as depicted in Figure 6 (a)-(c). Notably, Hierarchical clustering demonstrates the greatest diversity in cluster sizes, with the highest cluster containing 689 data points for the slug flow regime, while K-means and Gaussian clustering exhibit more uniformity. Specifically, K-means allocates 458 data points to Cluster 1, Gaussian assigns 440, and Hierarchical only 158, indicating disparities in their categorization approach. Moreover, Hierarchical clustering assigns 491 data points to Cluster 2, while Gaussian assigns 273 and K-means 365, further accentuating distinctions. Gaussian clustering tends to allocate more points to the annular flow cluster, with 580 data points, compared to K-means (442). These disparities underscore the importance of selecting an appropriate clustering algorithm based on the specific characteristics of the flow boiling regimes under study. While the total counts remain consistent, understanding the nuances of cluster distribution offers valuable insights into the underlying structure of the data and facilitates informed decision-making in analysing flow boiling regimes. Examining the two different flow types in the slug [red spots, (d)-(f)] and annular (blue spots, [(g)-(i)], which are often the most desired flow regimes for high heat transfer. For K-means at the same image and instance, it focuses more on the bubble separations, whilst GMM categorises the region between bubble separation and coalescence efficiently, but Hierarchical considers merges bubbles into the same category as during dry out. Although the differences in the overall images are minimal, these small differences compound and ultimately lead to the distinctions of clusters overall and affect the efficacy of the algorithms.

C. Comparatively Analysis

To conduct a detailed quantitative discussion on the findings based on the training and validation accuracy of the four different models, the trends and data insights are presented in Table 1.

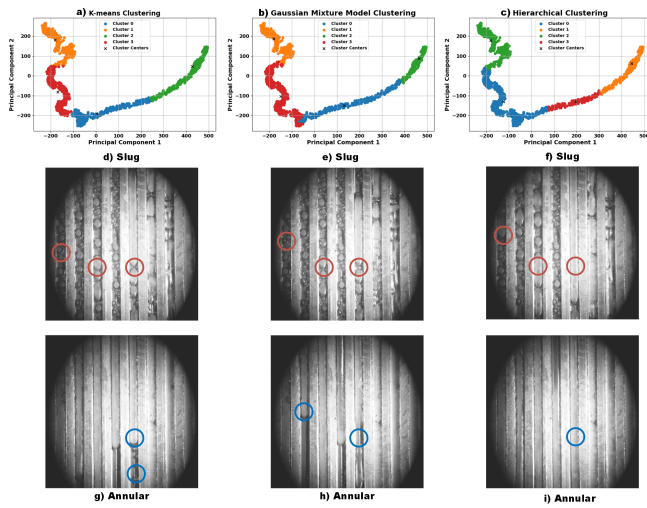


Fig. 6. Clustering output analysis

TABLE I
MODEL METRICS

Model	Metric	Mean	Median	SD
KMeans	Training Accuracy	0.8788	0.8879	0.0432
	Validation Accuracy	0.6198	0.6226	0.1232
Base CNN	Training Accuracy	0.9743	0.9749	0.0061
	Validation Accuracy	0.7706	0.7816	0.0504
GMM	Training Accuracy	0.9142	0.9195	0.0323
	Validation Accuracy	0.8837	0.8994	0.0538
Hierarchical	Training Accuracy	0.9013	0.9088	0.0310
	Validation Accuracy	0.7364	0.7166	0.0796

1. Dataset 1 (Base CNN, manually labelled data): Training Accuracy: Ranging from 0.9590 to 0.9848 Validation Accuracy: Ranging from 0.6709 to 0.8544

Key points:

- The training accuracy is relatively high, suggesting that the model performs well on the train set, but there are potential overfitting issues.
- There is less variance in validation accuracy compared to training accuracy, indicating good generalisation, as indicated by the standard deviation (SD) values.
- The model appears to converge quickly to high accuracy, suggesting that the dataset might be less complex or suited for the model architecture.

2. Dataset 2 (K-means, unlabelled data): Training Accuracy: Ranging from 0.7832 to 0.9275 Validation Accuracy: Ranging from 0.2767 to 0.8050

Key points:

- There is a notable discrepancy between training and validation accuracy, especially in the earlier epochs, indicating potential overfitting.
- The model achieves the lowest training accuracy and struggles to generalise well to the validation set, suggesting that the model might be too complex for the algorithm.
- The validation accuracy shows considerable variance, indicating potential instability in model performance.

3. Dataset 3 (GMM, unlabelled data): Training Accuracy: Ranging from 0.8384 to 0.9514 Validation Accuracy: Ranging from 0.7547 to 0.9686

Key points:

- The training and validation accuracy is relatively close, indicating that the model is not severely overfitting or underfitting.
- The validation accuracy is consistently high across epochs, indicating that the model generalises well to unseen data.
- There is a slight fluctuation in training and validation accuracy, which suggests the model might still benefit from further optimisation.

4. Dataset 4 (Hierarchical, unlabelled data): Training Accuracy: Ranging from 0.8389 to 0.9450 Validation Accuracy: Ranging from 0.6433 to 0.9363

Key points:

- The model exhibits a moderate level of overfitting as training accuracy is consistently higher than validation accuracy.
- The validation accuracy varies widely, indicating potential sensitivity to hyperparameters or dataset characteristics.
- Despite the overfitting, the model achieves decent validation accuracy, suggesting that it captures meaningful patterns in the data.

In terms of overall performance, the Gaussian Mixture Model offers the most stable and promising performance, with both high training and validation accuracy. The manually labelled base CNN also shows decent performance, although slight fluctuations suggest room for improvement. Hierarchical clustering exhibits overfitting but still achieves decent validation accuracy, indicating that the model might be capturing relevant features despite the noise. K-means shows the most erratic behaviour with a significant gap between training and validation accuracy, suggesting issues with model generalisation and potential overfitting. Nevertheless, while GMM appears to be the most promising based on the provided metrics, further analysis, including testing on unseen data and possibly experimenting with different model architectures or hyperparameters, would be necessary to make definitive conclusions about the dataset's suitability for the intended task.

D. Future Research Recommendation

This research was significant in advancing thermal management in microchannel heat sinks by tackling the challenge of flow boiling pattern recognition and streamlining inefficient data handling. It sheds light on effective classification techniques and presents practical approaches to enhance accuracy. Therefore, some potential avenues include: refining algorithms, exploring novel machine learning methods like Simple Contrastive Learning (SimCLR) or Physics-informed Neural Network-based (PINN) pattern recognition, and investigating the influence of operating conditions and heat sink designs. These findings are invaluable to the industry, enabling the

development of more efficient cooling systems and facilitating rapid, precise pattern recognition in real-world scenarios. Furthermore, this research holds the promise of driving innovation and elevating thermal management practices across various industries.

V. CONCLUSION

In conclusion, this research provided valuable insights into recognising flow boiling patterns within rectangular micro/mini channel heat sinks. Through systematic analysis and methodological refinement, the Gaussian Mixture Model clustering-based Convolutional Neural Network (CNN) approach demonstrated superior performance, achieving a mean accuracy of 91.4% on the training set and 88.4% on the test/validation set, with minimal variations and overfitting. Conversely, the K-means clustering approach exhibited the poorest performance, with a mean validation accuracy dropping as low as 62% and the highest variations within epochs, underscoring its inability to accurately identify complex underlying flow boiling patterns. Additionally, the research methodology facilitated the creation of an agile semi-automatic data pipeline, aiding accurate classification and expediting product development processes. Consequently, these findings advanced the heat transfer and thermal management research space, and the study findings also provide opportunities for enhancing predictive analytics, safety protocols, and real-time monitoring in industrial settings — whilst reducing subjectivity and interpretability issues. Thus, this study laid the groundwork for further exploration and innovation in advancing thermal management practices.

ACKNOWLEDGMENT

The authors would like to thank the support received from the University of Hertfordshire, University of Westminster, and the organising committee of the ICPRS 2024.

REFERENCES

- [1] V. Y. S. Lee and T. G. Karayiannis, 'Influence of system pressure on flow boiling in microchannels', *International Journal of Heat and Mass Transfer*, vol. 215, p. 124470, Nov. 2023, doi: 10.1016/j.ijheatmasstransfer.2023.124470.
- [2] B. Yang *et al.*, 'Computer Vision and Machine Learning Methods for Heat Transfer and Fluid Flow in Complex Structural Microchannels: A Review', *Energies*, vol. 16, no. 3, p. 1500, Jan. 2023, doi: 10.3390/en16031500.
- [3] M. Harris, H. Wu, W. Zhang, and A. Angelopoulou, 'Overview of recent trends in microchannels for heat transfer and thermal management applications', *Chemical Engineering and Processing - Process Intensification*, vol. 181, p. 109155, Nov. 2022, doi: 10.1016/j.cep.2022.109155.
- [4] G. M. Hobold and A. K. da Silva, 'Machine learning classification of boiling regimes with low speed, direct and indirect visualization', *International Journal of Heat and Mass Transfer*, vol. 125, pp. 1296–1309, Oct. 2018, doi: 10.1016/j.ijheatmasstransfer.2018.04.156.
- [5] A. W. Chu, B. Y. Liu, C. L. Pan, D. H. Zhu, and E. X. Yang, 'Identification of boiling flow pattern in narrow rectangular channel based on TFA-CNN combined method', *Flow Measurement and Instrumentation*, vol. 83, p. 102086, Mar. 2022, doi: 10.1016/j.flowmeasinst.2021.102086.
- [6] J. Loyola-Fuentes, L. Pietrasanta, M. Marengo, and F. Coletti, 'Machine Learning Algorithms for Flow Pattern Classification in Pulsating Heat Pipes', *Energies*, vol. 15, no. 6, Art. no. 6, Jan. 2022, doi: 10.3390/en15061970.

- [7] B. Zhao, X. Wen, and K. Han, 'Learning Semi-supervised Gaussian Mixture Models for Generalized Category Discovery', in *2023 IEEE/CVF International Conference on Computer Vision (ICCV)*, Paris, France: IEEE, Oct. 2023, pp. 16577–16587, doi: 10.1109/ICCV51070.2023.01524.
- [8] L. Zhu, Z. Jhia Ooi, T. Zhang, C. S. Brooks, and L. Pan, 'Identification of flow regimes in boiling flow with clustering algorithms: An interpretable machine-learning perspective', *Applied Thermal Engineering*, vol. 228, p. 120493, Jun. 2023, doi: 10.1016/j.applthermaleng.2023.120493.
- [9] Z. Wu, X. Chen, Y. Mao, E. Li, X. Zeng, and J.-X. Wang, 'A deep learning algorithm with smart-sized training data for transient thermal performance prediction', *Case Studies in Thermal Engineering*, vol. 39, p. 102420, Nov. 2022, doi: 10.1016/j.csite.2022.102420.
- [10] S. M. Aqil Burney and H. Tariq, 'K-Means Cluster Analysis for Image Segmentation', *IJCA*, vol. 96, no. 4, pp. 1–8, Jun. 2014, doi: 10.5120/16779-6360.
- [11] X. Ran, Y. Xi, Y. Lu, X. Wang, and Z. Lu, 'Comprehensive survey on hierarchical clustering algorithms and the recent developments', *Artif Intell Rev*, vol. 56, no. 8, pp. 8219–8264, Aug. 2023, doi: 10.1007/s10462-022-10366-3.
- [12] R. Al-batat, A. Angelopoulou, S. Premkumar, J. Hemanth, and E. Kapetanios, 'An End-to-End Automated License Plate Recognition System Using YOLO Based Vehicle and License Plate Detection with Vehicle Classification', *Sensors*, vol. 22, no. 23, Art. no. 23, Jan. 2022, doi: 10.3390/s22239477.
- [13] H. Babar, H. Wu, and W. Zhang, 'Investigating the performance of conventional and hydrophobic surface heat sink in managing thermal challenges of high heat generating components', *International Journal of Heat and Mass Transfer*, vol. 216, p. 124604, Dec. 2023, doi: 10.1016/j.ijheatmasstransfer.2023.124604.
- [14] I. Muraina, 'Ideal Dataset Splitting Ratios in Machine Learning Algorithms: General Concerns for Data Scientists and Data Analysts', presented at the 7th International Mardin Artuklu Scientific Research Conference, Mardin, Turkiye, Feb. 2022, pp. 496–504.
- [15] Z. Zhang and M. Sabuncu, 'Generalized Cross Entropy Loss for Training Deep Neural Networks with Noisy Labels', in *Advances in Neural Information Processing Systems*, Curran Associates, Inc., 2018.